This is a postprint version of the following published document:

Velasco, B., et al. (2016). Ti2AlC and Ti3SiC2 MAX Phase Foams: Processing, Porosity Characterization and Connection between Processing Parameters and Porosity. *World PM2016 Proceedings: Biomedical Applications*. EPMA, 2016
URL: https://www.epma.com/publications/euro-pm-proceedings/product/ep16-3296203

Ti$_2$AlC and Ti$_3$SiC$_2$ MAX Phase Foams: Processing, Porosity Characterization and Connection between Processing Parameters and Porosity

B. Velasco[1], T. Hutsch[2], T. Weißgärber[2], E. Gordo[1,] S.A. Tsipas[1]*

[1] *Departamento de Ciencia e Ingeniería de Materiales e Ingeniería Química, IAAB, Universidad Carlos III de Madrid, Avda. de la Universidad, 30, 28911 Leganés, Madrid, Spain.*
[2] *Fraunhofer Institute for Manufacturing and Advanced Materials, Dept. Sintered and Composite Materials, Winterbergstr. 28, D-01277 Dresden*
[*] *bvelasco@ing.uc3m.es*

ABSTRACT

MAX phases Ti$_2$AlC and Ti$_3$SiC$_2$ foams with controlled porosity and pore size were produced using the space holder method. The foams were processed using water-leachable crystalline carbohydrate as space holder that involves: mixing, cold isostatic pressing, dissolution and sintering. Three combinations of volume percentage (20%-60%) and size distribution (250-1000 µm) of space holder were introduced during mixing. The foams were characterized and compared with the material without space holder. The characterization included: morphology (overall, open and closed porosity by Archimedes method) and gas permeability. Foams with porosity up to about 60 vol% and pore size distribution ranging from about 250 to 1000 µm were produced. Experimental porosity was compared to the theoretical expected porosity. The results show a bimodal porosity that can be customized by the sintering and the space holder. This study connects the processing parameters to the porosity created and allows control of porosity and pore size to produce tailor-made properties.

Keywords: MAX phases, Ti$_2$AlC, Ti$_3$SiC$_2$, porous materials, eco-friendly processing, water-soluble space holder, permeability.

1. INTRODUCTION

MAX phases were first discovered in the 1967 by Jeitschko and Hans Nowotny [1, 2] but they were not studied in depth until the 90's by Barsoum [3]. The MAX phases are a new family of materials with remarkable properties which make them interesting for industry because they combine the properties of both metals and ceramics. MAX phases are ternary compounds generally denominated by the letters "M", "A", and "X" where: M is an early transition metal, A is an A-group element and X is carbon or nitrogen [4, 5]. They are combined stoichiometrically by the formula: $M_{n+1}AX_n$ where "n" is a number between 1 and 3. At the moment there are more than 60 MAX phases discovered. This study is focused on the Ti$_2$AlC and Ti$_3$SiC$_2$ MAX phases available commercially.

At the moment most of the research on Ti$_2$AlC and Ti$_3$SiC$_2$ MAX phases is focused in the solid material and there are few studies on porous material [6-22]. Porous MAX phases offer a better combination of properties than the conventional porous ceramics since they achieve good mechanical properties at high temperature in addition to being electrically and thermally conductive and also having excellent machinability. Porous MAX phases can find applications in: substrates for catalysts devices, porous electrodes, chemical filters, electrolyte clapboards, hot gas filtration, etc [23, 24]. Research in processing of porous materials is focused on flexibility in control of porosity from processing parameters that allows tuning the porosity to tailor-make the final foam properties.

This study is focused on controlling the porosity of the foams adjusting the processing parameters. The processing method employed is the space holder method in which the porosity is introduced by the space holder and controlled by modification of the space holder size and the powder/space holder ratio. The variation of porosity with the addition of space holder was studied in terms of open, closed and overall porosity and adjusted to a linear equation. The effect of pore size and amount of porosity on gas permeability was studied for both materials.

2. EXPERIMENTAL

Two commercial powders were employed: Ti_2AlC and Ti_3SiC_2 MAX phases from Sandvik (Sweden). Both were characterized. The average particle size was measured by Mastersizer 2000 equipment: D_{50}=9.801 µm for Ti_2AlC and D_{50}=5.582 µm for Ti_3SiC_2. The specific surface area was measured by using BET: 2.7674 m^2/g (Ti_2AlC) and 2.3670 m^2/g (Ti_3SiC_2). The density was determined using an Accupyc helium pycnometer: 4.122 g/cm^3 (Ti_2AlC) and 4.6970 for Ti_3SiC_2. After the powder characterization, the powders were mixed with 2% of lubricant (Acrowax C: $C_{38}H_{76}N_2O_2$, Lonza) to facilitate the compaction. The space holder was sieved into three size distributions: 250-400 µm, 400-800 µm, and 800-1000 µm. Then, three powder/space holder ratios in vol.% were mixed for each space holder size distribution resulting in nine different mixtures. Next, the mixtures were introduced inside a silicone mold and sealed. They were compacted by the cold uniaxial pressing (CIP) and pressed during 10 minutes at 400 MPa. The green bodies were soaked in distilled water under controlled conditions. Four conditions were studied in order to optimize the dissolution of the space holder. Then they were dried under controlled conditions: 30 °C during 24h. The samples were sintered in a vacuum furnace at 10^{-5} mbar. The thermal cycle included a 30 min plateau at 400 °C for delubrication purposes, and then they were sintered during 4 h at 1400 °C (Ti_2AlC) and at 1350 °C (Ti_3SiC_2). The samples were mechanized in a cylindrical shape with a lathe to obtain uniform geometry: constant diameter along the axe and plane-parallel bases. The porosity was calculated by Archimedes' method following the ASTM C20-00 standard and using ethanol to infiltrate the samples and as immersion medium. The samples were metallographically prepared: they were cut, inlayed in resin, grinded with SiC sandpaper and polished with diamond from 3 µm to 0.1 µm. Then, the samples' microstructure was observed by scanning electron microscope (SEM; Philips XL-30).

The gas permeability in the radial direction for each foam condition was determined using a special measuring cell. This equipment measures the permeability by emission of a flow of nitrogen gas through the probe. The pressure in the sample increases and is monitored. Each sample was drilled leaving a central hole (2mm in diameter). The gas permeability was calculated as the mass flow (Q) from the integration of the Forchheimer equation [25].

3. RESULTS AND DISCUSSIONS

Space holder elimination was monitored by measuring mass after the dissolution process in order to ensure complete space holder removal. The mass of the sample before and after dissolution was compared to the space holder mass content in the sample prior to dissolution, so a mass loss of 100% corresponds to complete removal of the space holder. Different dissolution conditions of temperature, time and stirring were compared (table 1). Condition 1, was studied only for Ti_2AlC, for which 71 % mass loss was achieved. Then, the temperature and time were raised, in condition 2, resulting in an elimination of 85% for Ti_3SiC_2 and an increase of 2% of mass loss for Ti_2AlC. Next, the time was increased up to 48h, in condition 3, and the mass loss achieved was: 96% for Ti_3SiC_2 and 85% for Ti_2AlC. Finally, stirring was added, in condition 4; and no significant variations were found for Ti_3SiC_2 and for Ti_2AlC 100% of mass loss was achieved. For Ti_3SiC_2 higher mass loss than Ti_2AlC was achieved under the same conditions without stirring.

Table 1. Details of dissolution conditions employed: time, temperature and stir.

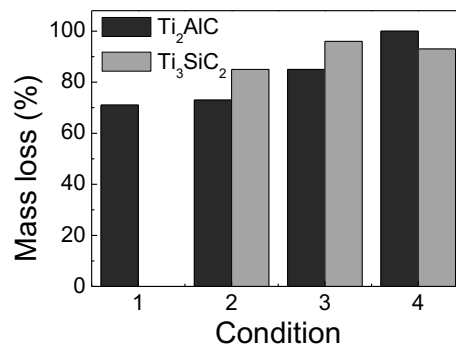| Leaching condition	Time (h)	Temperature (°C)	Stir
1	12	60	No
2	24	70	No
3	48	70	No
4	48	70	Yes

Figure 1. Variation of mass loss (%) of space holder after soaking under different dissolution conditions for Ti_2AlC and Ti_3SiC_2.

Figure 2 shows the results, for both materials, of porosity for the three amounts of space holder introduced in the mixture. The porosity was studied in terms of: open, closed and overall porosity. Ti_2AlC shows that porosity is mainly closed up to 40 vol.% of space holder and from 40 vol.% up to 60 vol.% of space holder, porosity is mostly open, for all space holder sizes. Ti_3SiC_2 exhibits mainly open porosity for all amounts of space holder and for all space holder size distributions. Porosity, for both materials, increases with the addition of space holder, and the addition of space holder increases open porosity. Moreover, all the foams have been compared with the material without space holder. Both materials show porosity in samples without space holder: 10 % and 32%, for Ti_2AlC and Ti_3SiC_2 respectively as a consequence of the processing parameters. This porosity appears in the cell walls of all processed foams and such porosity can be tuned by variations on pressing and sintering conditions. This effect results in bimodal porosity in the foams.
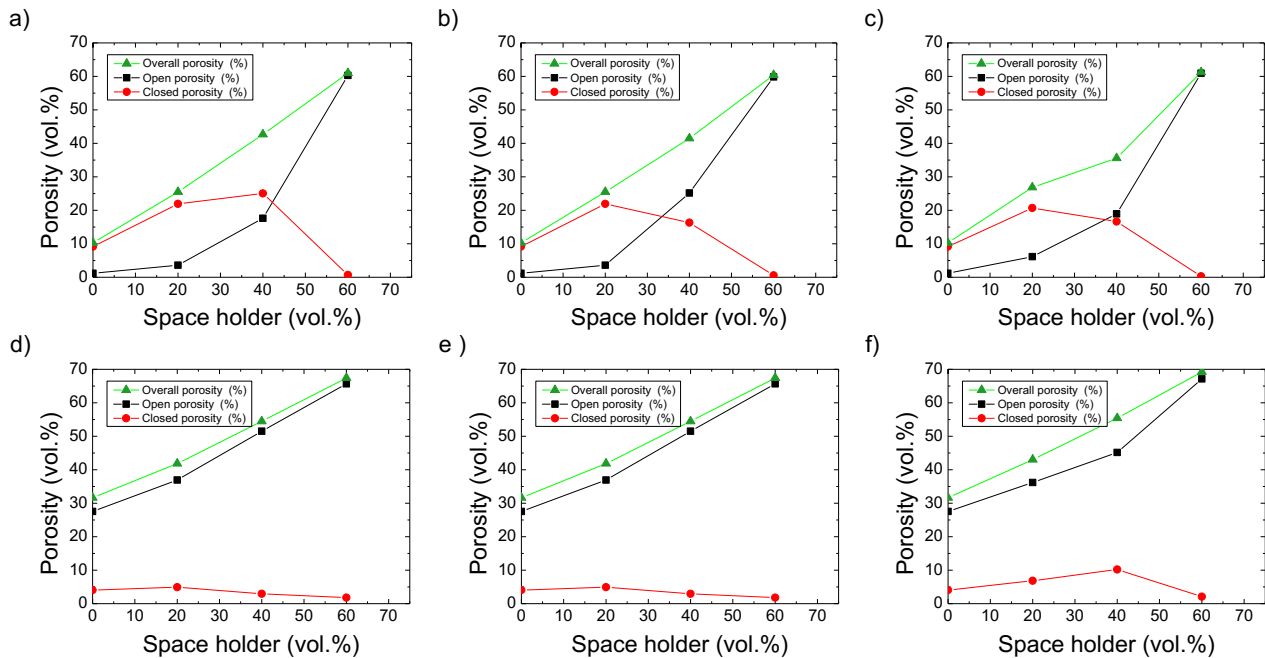

Figure 2. Variation of closed, open and overall porosity (vol.%) with the space holder (vol.%) added in the powder mixture for: a) Ti_2AlC and 250-400 µm of space holder size distribution, b) Ti_2AlC and 400-800 µm of space holder size distribution; c) Ti_2AlC and 800-1000 µm of space holder size distribution; d) Ti_3SiC_2 and 250-400 µm of space holder size distribution, e) Ti_3SiC_2 and 400-800 µm of space holder size distribution; f) Ti_3SiC_2 and 800-1000 µm of space holder size distribution.

Figure 3 shows representative micrographs of foams for both materials at different magnifications. Figures 3a and 3b show the porosity of the cell walls for Ti_2AlC and Ti_3SiC_2 respectively. Ti_3SiC_2 shows higher cell wall porosity and more interconnected pores, which is in agreement with the porosity measurement results that show a much higher porosity in Ti_3SiC_2 without space holder, as compared to Talc without space holder. This higher cell wall porosity might be responsible for the easier space holder dissolution observed in this foam. Representative microstructures of the foams are shown in figures 3c and 3d for both materials. It can be seen that pore morphology and distribution is similar and homogenous both materials. Overall appearance of the samples (figures 3e and 3f) is also similar and confirms that foams are well consolidated and easy to machine.

The comparison between overall and the theoretical porosity, namely that created only by addition of space holder, is shown in figures 4a and 4b for Ti_2AlC and Ti_3SiC_2 respectively. For Ti_2AlC overall and theoretical porosity are similar, suggesting that most of the porosity is due to the addition of the space holder. Ti_3SiC_2 presents more differences between theoretical and observed porosity due to the fact that the foam cell walls present higher level of porosity. The bimodal porosity present in the foams is represented as: Mode 1, which is the cell wall porosity, related to the processing parameters and Mode 2, which is the porosity created due to the addition of space holder. For both materials, overall porosity tends to be closer to the theoretical one as the amount of space holder increases. This occurs because the porosity contribution from the foam walls (Mode 1) decreases as the solid area decreases with increasing porosity.

Table 2 shows the linear fitting for overall porosity variation with respect to the amount of the space holder for both materials and for each size distribution. The equations show the variation of the porosity with the space holder obeys a linear relationship with an accurate adjustment, R^2. These equations allow the determination the space holder needed to process foams with a specific porosity.
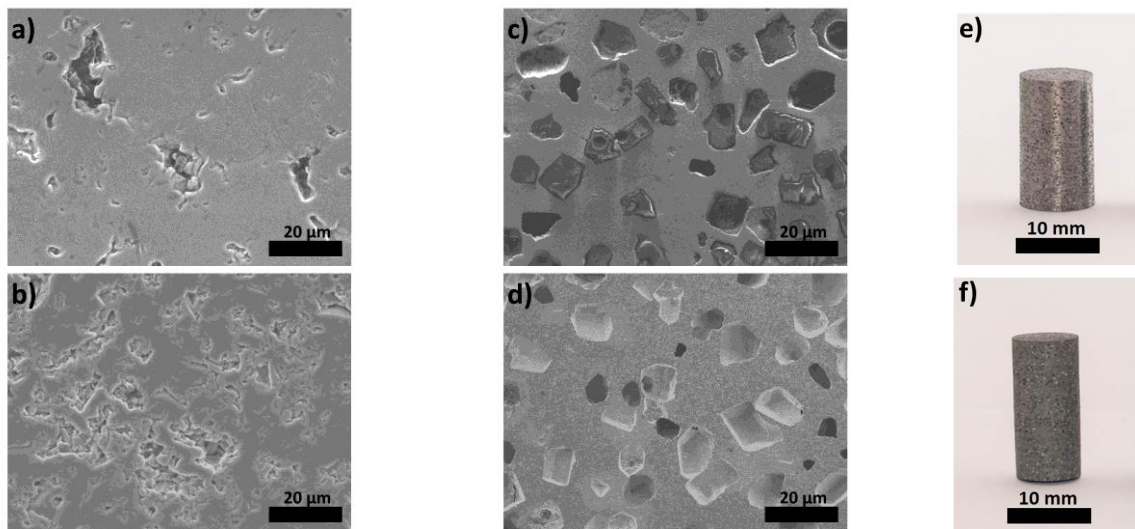

Figure 3. Representative microstructural features of foams of both materials (containing 40 vol.% and with 250-400 μm space holder size distribution) in three different magnifications: a) detail of cell wall for Ti_2AlC foam; b) detail of cell wall for Ti_3SiC_2 foam; c) characteristic foam microstructure for Ti_2AlC foam; d) characteristic foam microstructure for Ti_3SiC_2 foam; e) Ti_2AlC foam; f) Ti_3SiC_2 foam.
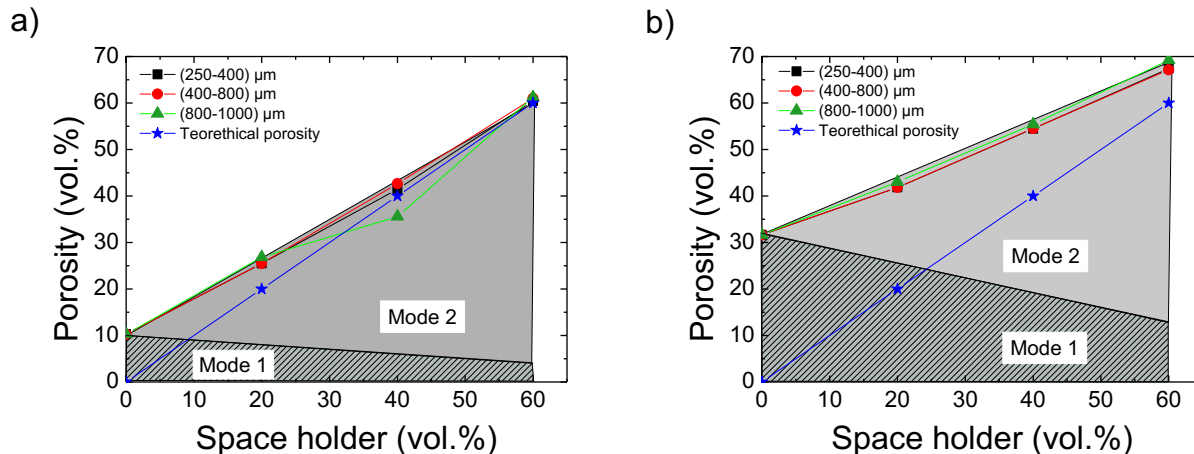

Figure 4. Variation of overall porosity (vol.%) with the addition of space holder (vol.%) in the mixture for the three space holder distributions (250-400 μm, 400-800 μm, and 800-1000 μm) for a) Ti_2AlC and b) Ti_3SiC_2. Moreover, both graphs distinguish the bimodal porosity: Mode 1: cell wall porosity and Mode 2: porosity due to the space holder.

Table 3 shows the gas permeability results for Ti_2AlC and Ti_3SiC_2 respectively for the three space holder size distributions. Both materials show increase in permeability with increasing porosity. Previous studies have demonstrated [26, 27], that porosity is the parameter with most influence on the permeability. This study has shown that the addition of space holder generates open porosity. For Ti_2AlC permeability is shown for porosity values higher than 35.57 vol.% since it was not possible to measure samples with lower porosities due to high overpressure. Samples with porosity lower than 35.57 vol.% have mainly closed porosity therewith, the gas flow through the sample is 0 and the gas permeability should be approximately 0 too. In Ti_3SiC_2 foam permeability is shown for all the samples since all of them have mainly open porosity. Ti_2AlC shows that for a fixed porosity (vol.%) the permeability is slightly higher for samples made with bigger space holder size distributions. The bigger space holder size leads to bigger pore sizes in the foam and increasing pore size increases the permeability [28]. Ti_3SiC_2 does not show clear tendency with the space holder size distribution. Ti_2AlC shows slightly higher permeability than Ti_3SiC_2 for the same porosity values. There are several parameters which affect to the permeability, the

most important are: porosity volume percentage, specific area and tortuosity. To get more conclusions about these results, specific area and tortuosity must to be determinated and studied.

Table 2. Linear relationship between the overall porosity (vol.%) the addition of space holder (vol.%), x, for three different size distributions and the quadratic adjustment R^2. Results for: Ti_2AlC and Ti_3SiC_2 materials.

Material	Space holder size distribution (µm)	Equation	R^2
Ti_2AlC	250-400	y=0.8204x+10	0.9971
	400-800	y=0.8349x+10	0.9980
	800-1000	y=0.7757x+10	0.9815
Ti_3SiC_2	250-400	y=0.6054x+32	0.9964
	400-800	y=0.5725x+32	0.9951
	800-1000	y=0.6054x+32	0.9964

Table 3. Variation of gas permeability, k, with the addition of space holder in the mixture and the porosity present in the foam for three space holder size distributions: 250-400 µm, 400-800 µm, and µm and 800-1000 µm for both materials Ti_2AlC and Ti_3SiC_2.

Material	Space holder (vol.%)	Space holder size distribution (250-400) µm		Space holder size distribution (400-800) µm		Space holder size distribution (800-1000) µm	
		Overall porosity (vol.%)	k (m^2)	Overall porosity (vol.%)	k (m^2)	Overall porosity (vol.%)	k (m^2)
Ti_2AlC	40	41.5	2.3×10^{-18}	42.7	6.8×10^{-18}	35.6	6.0×10^{-18}
	60	60.4	6.3	61.0	3.8	61.3	7.4
Ti_3SiC_2	0	31.6	2.0×10^{-16}	31.6	2.0×10^{-16}	31.6	2.0×10^{-16}
	20	41.9	3.6×10^{-16}	41.7	3.9×10^{-16}	43.0	3.9×10^{-16}
	40	54.5	1.2×10^{-14}	54.5	1.2×10^{-15}	55.4	8.4×10^{-16}
	60	67.4	1.2	67.2	1.4	69.2	2.2

4. CONCLUSIONS

This work has achieved consolidated foams with controlled porosity. Space holder dissolution was optimized achieving 100% and 93% of mass loss for Ti_2AlC and Ti_3SiC_2 respectively. With the selection of space holder size distribution the pore size was modified while tuning the powder/space holder ratio the porosity percentage in the foam is controlled. The resulting porosity is bimodal: Mode 1 represents cell wall porosity and depends on the processing parameters and Mode 2 depends on the amount of space holder. The porosity created by the addition of space holder in the mixture has been fitted to a linear equation with accuracy of R^2 of 0.99. The equation depends on the material and the space holder size distribution. The gas permeability has been studied on samples with mainly open porosity. The gas permeability depends on the porosity volume percentage, specific area and tortuosity.

5. ACKNOWLEDGMENTS

6. REFERENCES

[1] Nowotny H. Strukturchemie einiger Verbindungen der Übergangsmetalle mit den elementen C, Si, Ge, Sn. Progress in Solid State Chemistry. Volume 5, pages 27-70, 1971.
[2] Nowotny H., Rogl P, and Schuster J.C. Structural chemistry of complex carbides and related compounds. Volume 44 (1), pages: 126-133, 1982.
[3] Barsoum M. W. and El-Raghy T. Synthesis and characterization of a remarkable ceramic: Ti3SiC2. Journal of the American Ceramic Society. Volume 79, pages 1953–56 1996.
[4] Barsoum M.W. The M(N+1)AX(N) phases: a new class of solids: thermodynamically stable nanolaminates. Progress in Solid State Chemistry. Volume 28, pages 201–281, 2000.

[5] Radovic M., and Barsoum M.W. MAX phases: bridging the gap between metals and ceramics. American Ceramic Society Bulletin. Volume 92, pages, pages. 20–27, 2013.

[6] Fraczkiewicz M., Zhou A.G., and Barsoum M.W. Mechanical damping in porous Ti3SiC2 Acta Materialia Volume 54 (19), pages 5261–5270, 2006.

[7] Hu L., Benitez R., Basu S., Karaman I., and Radovic M. Processing and characterization of porous Ti2AlC with controlled porosity and pore size. Acta Materalia. Volume 60 (18), pages 6266–6277, 2012.

[8] Sun Z.M., Murugaiah A., Zhen T., Zhou A., and Barsoum M.W. Microstructure and mechanical properties of porous Ti3SiC2. Acta Materialia. Volume 53 (16), pages 4359–4366, 2005.

[9] Zhou A.G., Barsoum M.W., Basu S., Kalidindi S.R., and El-Raghy T. Incipient and regular kink bands in fully dense and 10 vol.% porous Ti2AlC. Acta Materialia. Volume 54 (6), pages 1631–1639, 2006.

[10] Zhou C.I., Ngai T.V.L., Lu L., and Li Y.Y. Fabrication and characterization of pure porous Ti3SiC2 with controlled porosity and pore features. Materials Letters. Volume 131, pages 280–283, 2014.

[11] Sun Z., Liang Y., Li M., and Zhou Y. Preparation of Reticulated MAX-Phase Support with Morphology-Controllable Nanostructured Ceria Coating for Gas Exhaust Catalyst Devices. Journal of the American Ceramic Society. Volume 93 (99, pages 2591–2597, 2010.

[12] Firstov S.A., Gorban V.F., Ivanova I.I., and Pechkovskii E.P. Mechanical properties of porous Ti3SiC2/TiC, Ti3AlC2/TiC, and Ti4AlN3/TiN nanolaminates at 20 to 1300°C. Powder Metallurgy and Metal Ceramics. Volume 49, pages 414-423, 2010.

[13] Sun Z., Liang Y., Li M., and Zhou Y. Preparation of reticulated MAX-phase support with morphology-controllable nanostructured ceria coating for gas exhaust catalyst devices. Journal of the American Ceramic Society. Volume 93 (9), pages. 2591–2597, 2010.

[14] Firstov S.A., Pechkovsky E.P., Ivanova I.I., Brodnikovksy N.P., Gorban V.F., and Demidik A.N. High-Temperature Mechanical Properties of Powder Metallurgy: Porous Lightweight Titanium Nanolaminates. High Temperature Materials and Processes. Volume 25, pages 47-58, 2006.

[15] Brodnikovskii N.P., Burka M.P., Verbilo D.G., Demidik A.N., Ivanova I.I., Koval A.Y., et al. Structure and mechanical properties of porous titanosilicon carbide Ti3SiC2. Powder Metallurgy and Metal Ceramics. Volume 42, pages 424-432, 2003.

[16] Bowen C.R., and Thomas T. Macro-porous Ti2AlC MAX-phase ceramics by the foam replication method. Ceramics International. Volume 41 (9), pages 12178–12185, 2015.

[17] Cheng F., Kim S-M., and Reddy J.N. Computational modeling of the plastic-damage behavior of porous MAX phase with aligned ellipsoid-like pores under uniaxial compression. International Journal of Solids and Structures. Volume 63 (15), pages 121–138, 2015.

[18] Potoczek M., Guzi de Moraes E., and Colombo P. Ti2AlC foams produced by gel-casting. Journal of the European Ceramic Society. Volume 35 (9), pages 2445–2452, 2015.

[19] Velasco B., Gordo E., and Tsipas S.A. MAX phase Ti2AlC foams using a leachable space-holder material. Journal of Alloys and Compounds. Volume 646 (15), pages 1036–1042, 2015.

[20] Amini S., Ni C.Y., and Barsoum M.W. Processing, microstructural characterization and mechanical properties of a Ti2AlC/nanocrystalline Mg-matrix composite. Composites Science and Technology. Volume 69 (3–4), pages 414–420, 2009.

[21] Amini S., and Barsoum M.W. On the effect of texture on the mechanical properties of nanocrystalline Mg-matrix composites reinforced with MAX phases. Materials Science and Engineering: A. Volume 527 (16–17), pages 3707-3718, 2010

[22] Kontsos A., Loutas T., Kostopoulos V., Hazeli K., Anasori B., and Barsoum M.W. Nanocrystalline Mg-MAX composites: mechanical behavior characterization via acoustic emission monitoring. Acta Materalia, 59 (14), pages 5716–5727, 2011.

[23] Ren XT, Zeng LK, and Wang H. The preparation technology of clay ceramics. Fushan Ceramics. Volume 5, pages 5-7, 2000.

[24] Ren XT, Zeng LK, and Wang H. Investigation of the preparation technology of foam ceramics. Materials Science and Engineering. Volume 19 (1), page 102–103, 2001.

[25] Forchheimer P. Wasserbewegung durch Boden. Zeitschrift des Vereins Deutscher Ingenieuer. 45, pages 1782-1788, 1901.

[26] Koponen A., Kataja M., and Timonen J. Permeability and effective porosity of porous media. Physical Review E. Volume 56, pages 3319-3329, 1997.

[27] Henderson N., Brettas J.C., and Sacco W.F., A three-parameter Kozeny–Carman generalized equation for fractal porous media. Chemical Engineering Science. Volume 65, pages 4432-4442, 2010.

[28] Bonnet J.-P., Topin F., Tadrist L. Flow Laws in Metal Foams: Compressibility and Pore Size Effects. Transport in Porous Media. Volume 73, pages 233–254, 2008.